CCC 2008 - Challenges for Civil Construction
Torres Marques et al. (Eds)

BEHAVIOUR OF RC BEAMS SHEAR STRENGTHENING WITH NSM CFRP LAMINATES

Salvador J.E. Dias[1] and Joaquim A.O. Barros[2]

ISISE, School of Engineering, University of Minho
Campus de Azurem, 4800-058 Guimarães, Portugal
e-mail: [1]sdias@civil.uminho.pt, [2]barros@civil.uminho.pt
web page: http://www.civil.uminho.pt/composites

Keywords: NSM, EBR, CFRP laminates, strips of wet lay-up CFRP sheets, shear strengthening, T cross section reinforced concrete beams.

Summary: *The effectiveness of the Near Surface Mounted (NSM) technique with Carbon Fiber Reinforced Polymer (CFRP) laminates for the shear strengthening of T cross section reinforced concrete (RC) beams is assessed by experimental research. The influence of the percentage and inclination of CFRP laminates on the shear strengthening contribution was evaluated. The experimental program also includes beams strengthened according to the externally bonded reinforcement (EBR) technique in order to compare the effectiveness of NSM and EBR shear strengthening strategies.*

1 INTRODUCTION

Near surface mounted (NSM) is a relatively recent strengthening technique of high potential to increase the shear resistance of reinforced concrete (RC) beams that have some risk of collapsing in a brittle shear failure mode. NSM is based on introducing Carbon Fiber Reinforced Polymer (CFRP) bars into slits opened on the concrete cover of the lateral faces of the beam. CFRP bars of circular [1], square [2] and rectangular [3] cross section have been used for the NSM shear strengthening of RC beams. Due to the largest bond area and higher confinement provided by the surround concrete, CFRP laminates installed into thin slits and bonded to concrete by an epoxy adhesive are proved as being the most effective CFRP strengthening elements for the NSM shear strengthening of RC beams [4]. The effectiveness of the NSM technique for the shear strengthening of rectangular cross sectional RC beams was already well proved [5]. The effectiveness of the NSM for the shear strengthening of T cross section RC beams was recently explored carrying out series of tests with beams of concrete of low, medium and relatively high compressive strength [6-8].

NSM requires no surface preparation work and, after cutting the slit, requires minimal installation time compared to the Externally Bonded Reinforcing (EBR) technique. A further advantage associated with NSM is its ability to significantly reduce the probability of harm resulting from acts of vandalism, mechanical damages and aging effects. When NSM is used, the appearance of a structural element is practically unaffected by the strengthening intervention. However, the effectiveness of the EBR and NSM for the shear strengthening of T cross section RC beams having a certain percentage of steel stirrups was not yet well explored. The present work is dedicated to the comparison of shear strengthening effectiveness provided by these both techniques, as well as to the evaluation of the influence of percentage and inclination of laminates in terms of the NSM shear strengthening performance. A detailed description of the carried out experimental research and a discussion of the obtained results is done in the present paper.

2 EXPERIMENTAL PROGRAM

2.1 Test series, test set up and monitoring system

Figure 1 presents the T cross section of the fifteen beams comprising the experimental program. The reinforcement systems were designed to assure shear failure mode for all the tested beams. To localize shear failure in only one of the beam shear spans, a three point load configuration of a distinct length of the beam shear spans was selected, as shown in Figure 1. The monitored beam span (L_i) is 2.5 times the effective depth of the beam (L_i/d=2.5). To avoid shear failure in the L_r beam span, steel stirrups ϕ6@75mm were applied in this span. The differences between the tested beams are restricted to the shear reinforcement systems applied in the L_i beam span. The experimental program (see Table 1) is made up of one beam without any shear reinforcement (C-R beam); one beam with steel stirrups ϕ6@300mm (2S-R beam with a percentage of steel stirrups, ρ_{sw}, of 0.10%); one beam with steel stirrups ϕ6@112.5mm (7S-R beam with ρ_{sw} =0.28%); and twelve beams of ϕ6@300mm. These last beams also include distinct CFRP arrangements on the L_i beam span (see Table 1): nine beams with NSM laminates (three distinct percentages of CFRP laminates and, for each CFRP percentage, three inclinations for the laminates, 90º, 60º and 45º); and three beams with strips of unidirectional CFRP wet lay-up sheets of a U configuration.

The CFRP shear strengthening percentage, ρ_{fw}, was obtained from:

$$\rho_{fw} = \frac{2 \cdot a_f \cdot b_f}{b_w \cdot s_f \cdot sen\theta_f} \tag{1}$$

where a_f = 1.4 mm and b_f = 9.5 mm are the dimensions of the laminate cross section. In equation (1), b_w = 180 mm is the beam web width, and s_f and θ_f represent the spacing and inclination of the laminates, respectively. In the case of beams strengthened according to the EBR technique, a_f = 0.176 mm and b_f = 60 mm are the thickness and the width of the wet lay-up strips of CFRP sheet.

For the three series of NSM strengthened beams, with laminates of distinct orientations, the highest ρ_{fw} in each series was evaluated to assure that the corresponding beams had a maximum load similar to the beam reinforced with the highest ρ_{sw} (ϕ6@112.5mm in the shortest beam's span, the 7S-R beam). In the evaluation of the maximum ρ_{fw}, it was assumed that CFRP works like a steel stirrup. However, instead of considering the yield stress of the material, a stress in the laminates corresponding to a strain of 5.0% was adopted since this is a compromise between the maximum value recommended by ACI [9] for the EBR (4.0‰), and the 5.9‰ value obtained in pullout bending tests with NSM strengthening technique using CFRP laminates [10]. Following this approach, the arrangements indicated in Table 1 and Figure 2 were adopted: ten laminates in each of the beam lateral faces for θ_f =90º and θ_f =45º; nine laminates in each of the beam lateral faces for θ_f =60º. For the lowest and intermediate ρ_{fw}, the s_f for each θ_f (90º, 60º and 45º) was obtained with the purpose that the contribution of the CFRP would be similar. Independent from laminate orientation for beams with the lowest ρ_{fw}, four laminates were applied on each lateral face of the beam. For the intermediate ρ_{fw} seven laminates in each of the beam lateral faces for θ_f =90º and θ_f =45º and six laminates for θ_f =60º were applied. For the EBR strengthened, the percentages of discrete strips of wet lay-up CFRP sheet were evaluated in order to assure, according to the formulation recommended by ACI [9], the same load carrying capacity of the corresponding NSM strengthened series of beams (see Table 1 and Figure 2).

The laminates and the strips of sheet were distributed along the AB line represented in Figure 1, where A represents beam support at its "test side" and B is obtained assuming a load degradation at 45º.

The three point beam bending tests (Figure 1) were carried out using a servo closed-loop control equipment, taking the signal read in the displacement transducer (LVDT), placed at the loaded section, to control the test at a deflection ratio of 0.01 mm/s. To avoid concrete spalling at the most loaded beam support, a confinement system based on the use of wet lay-up CFRP sheets was applied according to the configuration illustrated in Figure 1. With the purpose of obtaining the strain variation along the laminates and strips of sheet that have the highest probability of providing the largest contribution for the shear strengthening of the RC beam, four strain gauges (SG_L in laminates and SG_M in the strips of sheet) were bonded in each CFRP according to the arrangement represented in Figure 3. Adopting the same principle, one steel stirrup was monitored with three strain gauges (SG_S) installed according to the configuration represented in Figure 3. The location of the monitored laminates, strips of sheet and stirrups in the tested beams is represented in Figure 2.

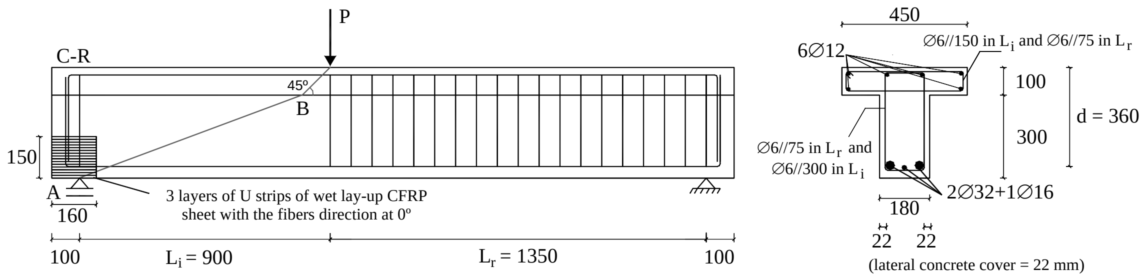

Figure 1: Tested beams: geometry, steel reinforcements applied in all beams and CFRP-based strengthening configuration of the most loaded beam support (dimensions in mm)

Table 1: CFRP shear reinforcement configurations of the tested beams

Beam	CFRP shear reinforcement system in the smaller beam shear span (L_i)				
	Shear strengthening	Quantity	Percentage (%)	Spacing (mm)	Angle [d] (º)
2S-4LV	NSM CFRP laminates	2x4 laminates (1.4x9.5 mm^2)	0.08	180	90
2S-7LV		2x7 laminates (1.4x9.5 mm^2)	0.13	114	90
2S-10LV		2x10 laminates (1.4x9.5 mm^2)	0.18	80	90
2S-4LI45		2x4 laminates (1.4x9.5 mm^2)	0.08	275	45
2S-7LI45		2x7 laminates (1.4x9.5 mm^2)	0.13	157	45
2S-10LI45		2x10 laminates (1.4x9.5 mm^2)	0.19	110	45
2S-4LI60		2x4 laminates (1.4x9.5 mm^2)	0.07	243	60
2S-6LI60		2x6 laminates (1.4x9.5 mm^2)	0.11	162	60
2S-9LI60		2x9 laminates (1.4x9.5 mm^2)	0.16	108	60
2S-4M [a]	EBR CFRP wet lay-up sheets	4 strips of CFRP wet lay-up sheets U configuration - 1 layer (0.176x60 mm^2)	0.07	180	90
2S-7M(1) [b]		7 strips of CFRP wet lay-up sheets U configuration - 1 layer (0.176x60 mm^2)	0.10	114	90
2S-7M(2) [c]		7 strips of CFRP wet lay-up sheets U configuration - 2 layers (0.176x60 mm^2)	0.21	114	90

a The predicted load carrying capacity of this beam was similar to the 2S-4LV, 2S-4LI45 and 2S-4LI60 beams; b The predicted load carrying capacity of this beam was similar to the 2S-7LV, 2S-7LI45 and 2S-6LI60 beams; c The predicted load carrying capacity of this beam was similar to the 2S-10LV, 2S-10LI45 and 2S-9LI60 beams; d Angle between the CFRP fiber direction and the beam axis.

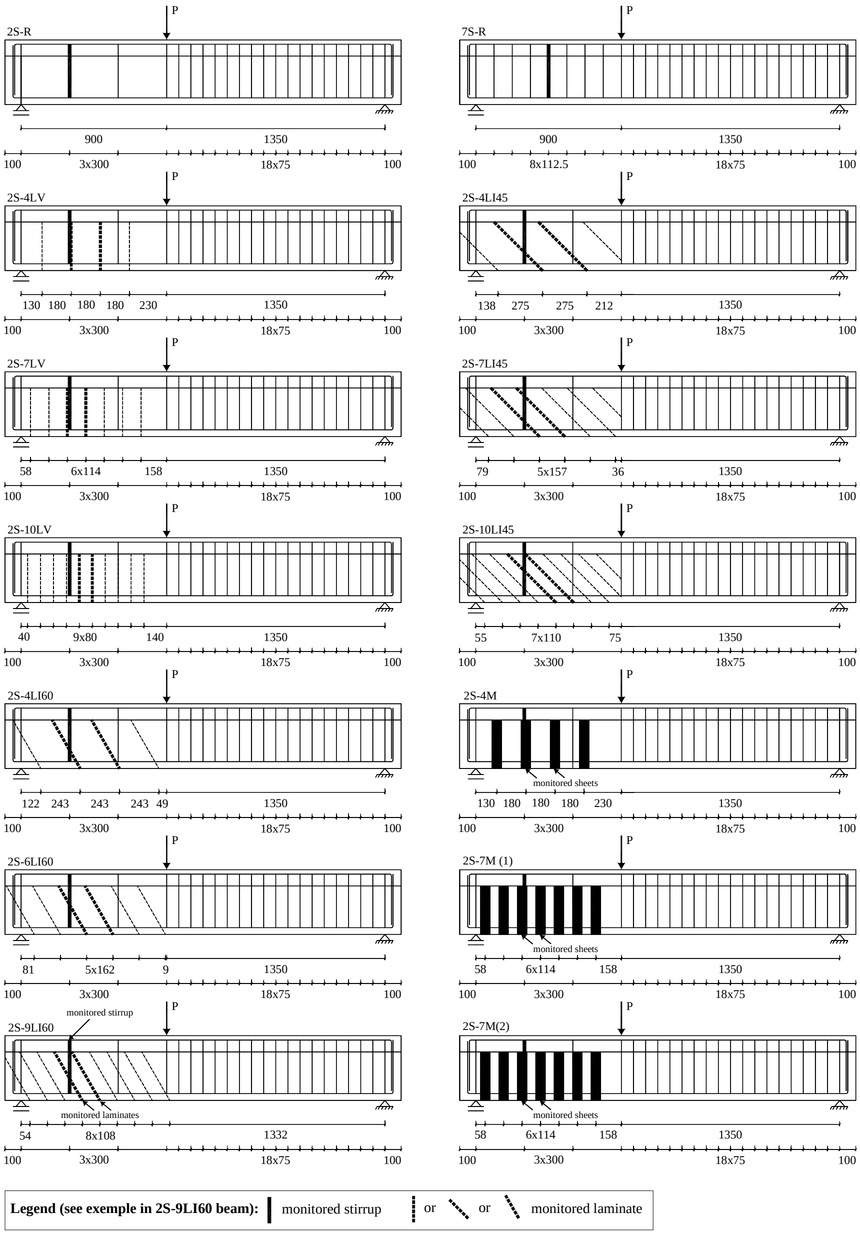

Figure 2: Localization of the steel stirrups (thick line), CFRP laminates (dashed line) and strips of CFRP sheets in the tested beams (dimensions in mm)

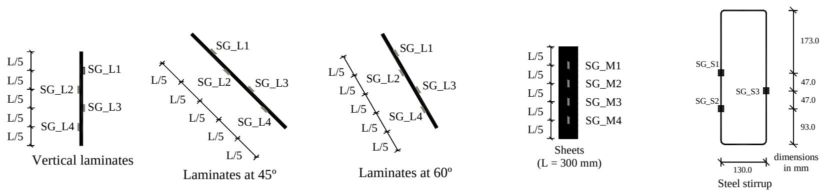

Figure 3: Positions of the strain gauges in the laminate, strip of sheet and stirrup

2.2 Material properties

The concrete compressive strength was evaluated at 28 days and at the age of the beam tests, carrying out direct compression tests with cylinders of 150 mm diameter and 300 mm height, according to EN 206-1 [11]. In the tested beams, high bond steel bars of 6, 12, 16 and 32 mm diameter were used. The values of their main tensile properties were obtained from uniaxial tension tests performed according to the recommendations of EN 10002 [12]. The properties of the CFK 150/2000 S&P laminates, under tension, were characterized by uniaxial tension tests carried out according to ISO 527-5 [13]. Table 2 includes the average values obtained from these experimental programs. The tensile properties of the wet lay-up CFRP sheet, with the designation, S&P C240 - 300g/m^2, was characterized elsewhere [14]. The S&P Resin 220 epoxy adhesive was used to bond the laminates to the concrete, while S&P Resin 50/55 was applied to bond the wet lay up strips of CFRP sheets. The characteristics of these adhesives can be consulted in http://www.sp-reinforcement.ch/datasheets.htm.

Table 2: Values of the properties of intervening materials

Concrete	Compressive strength				
	f_{cm} = 31.7 MPa (at 28 days)			f_{cm} = 39.7 MPa (at 106 days - age of beam tests)	
Steel	Tensile strength	ϕ6	ϕ12	ϕ16	ϕ32
	f_{sym} (yield stress)	542 MPa	453 MPa	447 MPa	759 MPa
	f_{sum} (maximum stress)	594 MPa	591 MPa	566 MPa	902 MPa
CFRP Laminates	Maximum tensile strength	Young's Modulus	Maximum strain	Thickness	
	f_{fum} = 2952 MPa	E_{fm} = 166.6 GPa	ε_{fu} = 17.7 ‰	1.4 mm	
Wet lay up CFRP sheet	Maximum tensile strength	Young's Modulus	Maximum strain	Thickness	
	f_{fum} = 2862.9 MPa	E_{fm} = 218.4 GPa	ε_{fu} = 13.3 ‰	0.18 mm	

2.3 Strengthening technique

The NSM strengthening technique is composed of the following procedures: 1) using a diamond cutter, slits of about 4-5 mm width and 12-15 mm depth were opened on the concrete cover (of about 22 mm thickness) of the lateral faces of the beam web, according to the pre-defined arrangement for the laminates (the laminates were not anchored to the beam flange; they were restricted to the beam web); 2) the slits were cleaned by compressed air; 3) the laminates were cleaned with acetone; 4) the epoxy adhesive was produced according to the supplier recommendations; 5) the slits were filled with the adhesive; 6) the adhesive was applied on the faces of the laminates; and 7) the laminates were inserted into the slits and adhesive in excess was removed.

To apply the wet lay up strips of CFRP sheet by EBR technique, the following procedures were executed: 1) on the zones of the beams surfaces where the strips of sheet would be glued, an emery was applied to remove the superficial cement paste, and the beam's edges were rounded (with a radius of about 20 mm); 2) the residues were removed by compressed air; 3) a layer of primer was applied to regularize the concrete surface and to enhance the adherence capacity of the concrete substrate; and 4) using resin, the strips of sheet were glued on the faces of the beam.

To guarantee a proper curing of the adhesive, at least one week passed between the beam strengthening operations and the beam test.

2.4 Results and discussion

2.4.1 Load carrying capacity of the tested beams

Table 3 includes the maximum value of the ratio between the load increment provided by each shear strengthening system (ΔF), after the formation of the first shear crack in the 2S-R reference beam, and the corresponding load capacity of this reference beam (F^{2S-R}), see Figure 5, resulting in a parameter designated as strengthening efficacy index, $\left(\Delta F/F^{2S-R}\right)_{max}$. Table 3 also includes the deflection at the loaded section when $\left(\Delta F/F^{2S-R}\right)_{max}$ occurred, which is designated by $u_{\left(\Delta F/F^{2S-R}\right)_{max}}$. Assuming F_{max}, F_{max}^{2S-R} and F_{max}^{7S-R} to be the load carrying capacities (maximum force) of all the tested beams, of the 2S-R reference beam and of the 7S-R reference beam, respectively, the values of $\Delta F_{max}/F_{max}^{2S-R}$ and F_{max}/F_{max}^{7S-R} ratios are indicated in Table 3 ($\Delta F_{max} = F_{max} - F_{max}^{2S-R}$). The force *vs* deflection at the loaded-section (u_{LS}) relationship and the $\Delta F/F^{2S-R}$ *vs* u_{LS} relationship are depicted in Figure 4.

The results included in Table 3 and represented in Figure 4 show that, for deflections higher than the one registered at the formation of the shear failure crack in the 2S-R reference beam (2.15 mm), all the CFRP configurations provided an increase on the beam's load carrying capacity (the exception was 2S-7LV beam). In fact, the load decay observed in the 2S-R reference beam, when the shear failure crack was formed, did not occur in the CFRP shear strengthened beams, revealing that the CFRP delayed the formation and propagation of the shear crack. This results in an increase of beam stiffness after the deflection corresponding to the formation of the shear crack in the reference beam. The presence of the CFRP delayed the loss of the contribution of the concrete aggregate interlock for the concrete shear resistance, as well as the stage in which the stirrups entered their plastic phase.

The strengthening arrangements with the lowest ρ_{fw} had the smallest increments in terms of beam load carrying capacity ($\Delta F_{max}/F_{max}^{2S-R}$): 11.1%, 29.3% and 27.2% for the beams strengthened with vertical laminates (2S-4LV beam), at 45º (2S-4LI45 beam) and at 60º (2S-4LI60 beam), respectively, see Figure 4. In terms of $\left(\Delta F/F^{2S-R}\right)_{max}$ ratio, only 2S-4LV beam presented higher value than the one obtained for $\Delta F_{max}/F_{max}^{2S-R}$ (16.4%). For the lowest ρ_{fw}, the EBR shear configuration only provided an increase of 2.4% in the beam load carrying capacity of the 2S-R reference beam. However, the increase of $\left(\Delta F/F^{2S-R}\right)_{max}$ was much more pronounced (13%), showing that the strips of wet lay up CFRP sheets contributed for the increase of the stiffness of the beam after shear crack formation.

For the beams shear strengthened with the intermediate ρ_{fw}, the strengthening configurations of vertical laminates, laminates at 45º and laminates at 60º assured an increase in the beam load carrying capacity of 23.1%, 38.8% and 29.8%, respectively. The beams with the NSM intermediate ρ_{fw} presented $\Delta F_{max}/F_{max}^{2S-R} = \left(\Delta F/F^{2S-R}\right)_{max}$. For the intermediate ρ_{fw}, the EBR 2S-7M(1) beam presented a $\Delta F_{max}/F_{max}^{2S-R}$ =7.0% and a $\left(\Delta F/F^{2S-R}\right)_{max}$ =19.4%. After the formation of a shear crack in the 2S-R reference beam, the $\left(\Delta F/F^{2S-R}\right)_{max}$ and $\Delta F_{max}/F_{max}^{2S-R}$ values of these strengthened beams were more pronounced than the $\left(\Delta F/F^{2S-R}\right)_{max}$ and $\Delta F_{max}/F_{max}^{2S-R}$ values of the beams strengthened with the lowest ρ_{fw}.

Amongst the beams strengthened with the highest ρ_{fw}, as already happened for the other two percentages, the strengthening configuration of θ_f =45º was the most effective in terms of maximum load capacity, since an increase of 47% was obtained, while an increase of 30.8% and 35.8% was recorded for the strengthening arrangements of θ_f =90º and θ_f =60º, respectively. These increments were also registered for the $\left(\Delta F/F^{2S-R}\right)_{max}$. The EBR beam shear strengthened with the highest value of ρ_{fw} (2S-7M(2) beam) presented a $\Delta F_{max}/F_{max}^{2S-R}=\left(\Delta F/F^{2S-R}\right)_{max}$ =21.8%. Therefore, regardless the percentage and orientation of the laminates, the NSM technique was most effective than the EBR technique.

As already mentioned, the highest ρ_{fw} for each strengthening arrangement was designed to assure that the beams load carrying capacity was similar to that of the 7S-R reference beam. The maximum load of the NSM strengthened beams with θ_f =90º (2S-10LV), θ_f =45º (2S-10LI45) and θ_f =60º (2S-9LI60) had a maximum load of 85%, 96% and 88% of the maximum load of the 7S-R reference beam, respectively, see Figure 4 and Table 3, which correspond to an average increase of 90%. However, the maximum load of the 2S-7M(2) EBR beam was only 79% of the F_{max}^{7S-R}. The most notable aspect is, however, that after the shear crack initiation of the 2S-R beam, the strengthened beams with NSM demonstrated a larger load capacity than the 7S-R reference beam (see Figure 4). This improved performance of the strengthened beams derives from the stiffness contribution provided by the NSM CFRP strengthening elements. In fact, Figure 4 shows that, after shear crack initiation, the strengthened beams with NSM laminates exhibited stiffer behavior than that of the 7S-R beam.

With the exception of the highest ρ_{fw} the NSM technique was most effective than the EBR technique in terms of deformation capacity at beam failure.

Table 3: Relevant results in terms of the load capacity up to beam's failure

Beam	F_{max} (kN)	$\Delta F_{max}/F_{max}^{2S-R}$ (%)	F_{max}/F_{max}^{7S-R}	$\left(\Delta F/F^{2S-R}\right)_{max}$ (%)	$u_{\left(\Delta F/F^{2S-R}\right)_{max}}$ [a] (mm)
C-R	207.0	-	0.44	-	-(7.48)
2S-R	303.8	-	0.65	0.0	- (5.88)
7S-R	467.5	53.9	1.00	53.9	8.78 (8.78)
2S-4LV	337.4	11.1	0.72	16.4	4.65 (7.14)
2S-7LV	374.1	23.1	0.80	23.1	7.17 (7.17)
2S-10LV	397.5	30.8	0.85	30.8	6.09 (6.09)
2S-4LI45	392.8	29.3	0.84	29.3	6.45 (6.45)
2S-7LI45	421.7	38.8	0.90	38.8	7.93 (7.93)
2S-10LI45	446.5	47.0	0.96	46.9	6.74 (6.76)
2S-4LI60	386.4	27.2	0.83	27.2	6.90 (6.90)
2S-6LI60	394.4	29.8	0.84	29.8	7.77 (7.87)
2S-9LI60	412.7	35.8	0.88	35.8	6.44 (6.44)
2S-4M	311.1	2.4	0.67	13.0	3.78 (4.79)
2S-7M(1)	325.1	7.0	0.70	19.4	4.32 (5.99)
2S-7M(2)	370.1	21.8	0.79	21.8	7.77 (7.77)

a The value into rounded brackets is referred corresponds to the deflection at the loaded section when the maximum load occurs.

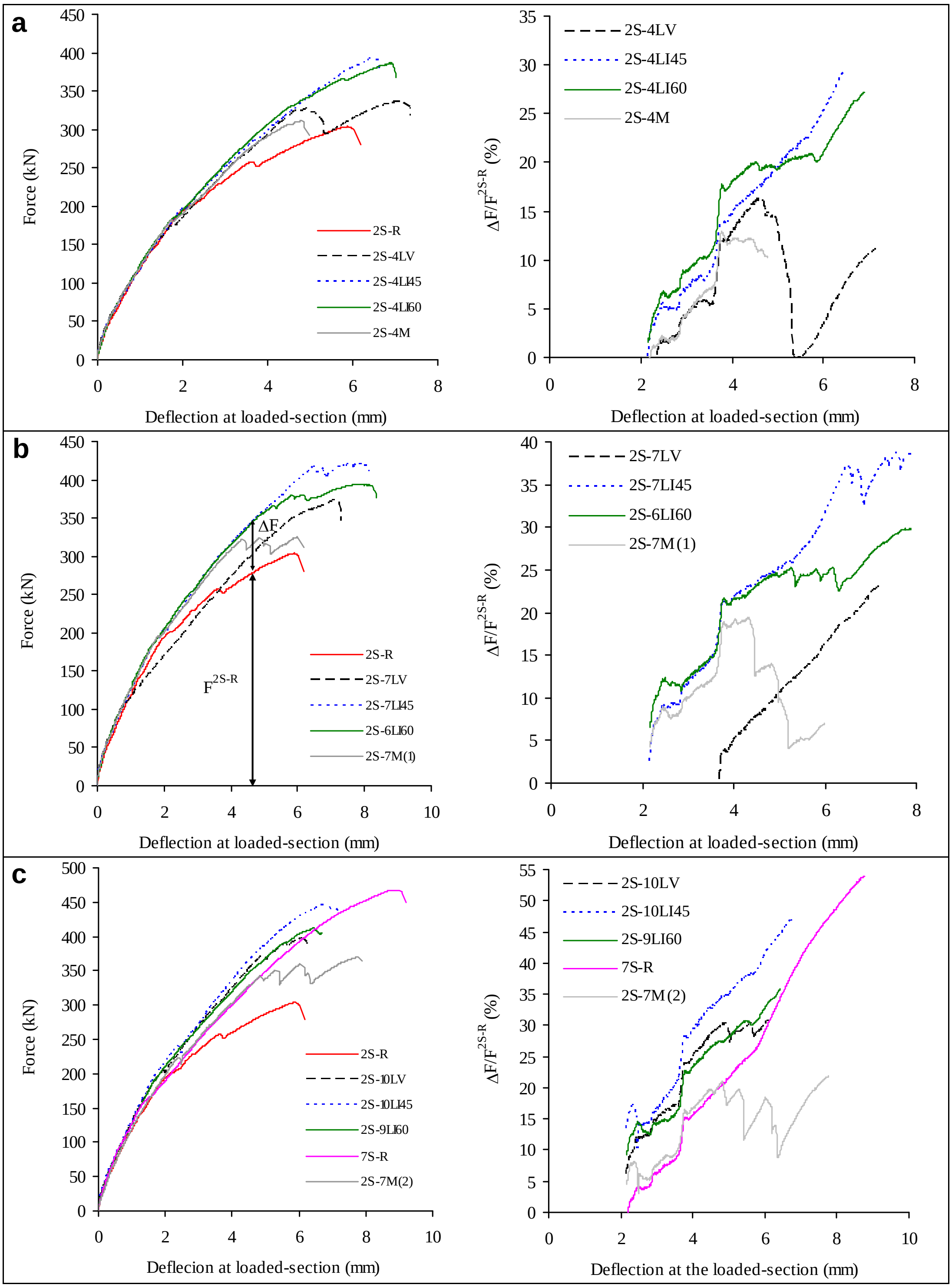

Figure 4: Force *vs* deflection at the loaded-section and $\Delta F/F^{2S-R}$ *vs* deflection at the loaded-section for the beams strengthened with the: a) lowest; b) intermediate; c) highest, percentage of CFRP shear strengthening

2.4.2 Failure modes

As expected, all beams failed in shear. Figure 5 includes details of the shear failure zones of all the tested beams (the steel stirrups at the smaller beam shear span are indicated by vertical lines, and the circles indicate the zone where stirrups ruptured, see also Figure 2).

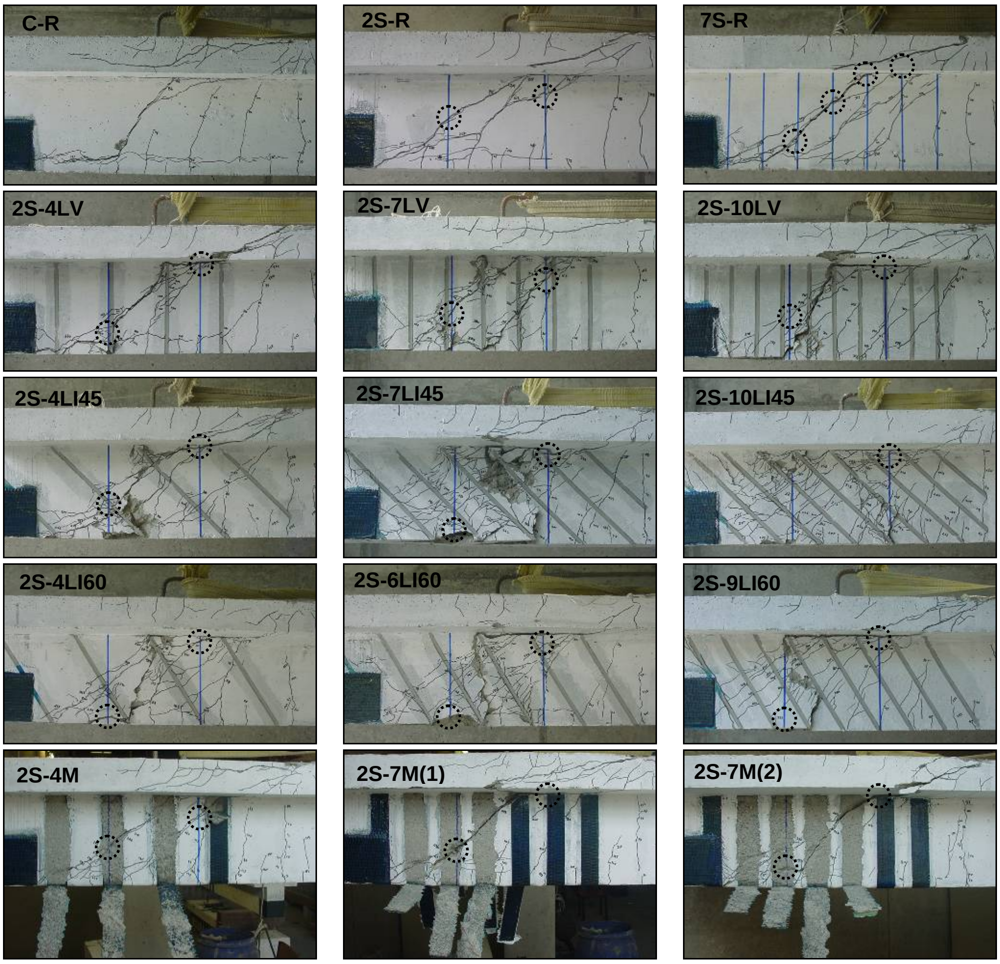

Figure 5: Details of the failure zone of the tested beams

In C-R beam, the shear crack wide intensively when the maximum load was attained. For the 2S-R and 7S-R beams, the maximum load was attained when one stirrup that crossed the shear failure crack ruptured.

In general, for the beams with the minimum ρ_{fw} the laminates failed by "debonding". However, in the present context, "debonding" should not be assumed as a pure debonding failure mode for the laminate, since along its "bond length", concrete adhered to the laminate, indicating that failure always occurred due to concrete fracture. In the beams with the intermediate ρ_{fw}, and mainly in beams with the largest ρ_{fw}, the typical failure mode is the separation of parts of the concrete cover, which was already observed in previous experimental programs [6-8]. The tendency for the occurrence of the detachment of the concrete cover indicates a detrimental effect between consecutive laminates (group effect), which has being efficiently taken into account in a innovative analytical model, able of predicting the contribution of the NSM laminates for the shear resistance of RC beams [15].

For the EBR beams (2S-4M, 2S-7M(1) and 2S-7M(2)) the failure mode was the debonding of wet lay up CFRP sheets from the concrete (see Figure 5). This failure mode was independent of the CFRP percentage.

2.4.3 Effect of the percentage and inclination of the CFRP

Figure 6 represents the relationship between the strengthening efficacy, $\Delta F_{max}/F_{max}^{2S-R}$, provided by the CFRP arrangements and the CFRP percentage (ρ_{fw}) for the analyzed NSM and EBR shear strengthening configurations (see Tables 1 and 3). This figure shows that, regardless the ρ_{fw}, the arrangement of laminates at 45º was the most effective among the adopted CFRP shear strengthening configurations, and the EBR was the lowest effective configuration. This figure shows also a trend of linear increasing of $\Delta F_{max}/F_{max}^{2S-R}$ with the increase of ρ_{fw}, for the range of ρ_{fw} values considered in the present experimental program.

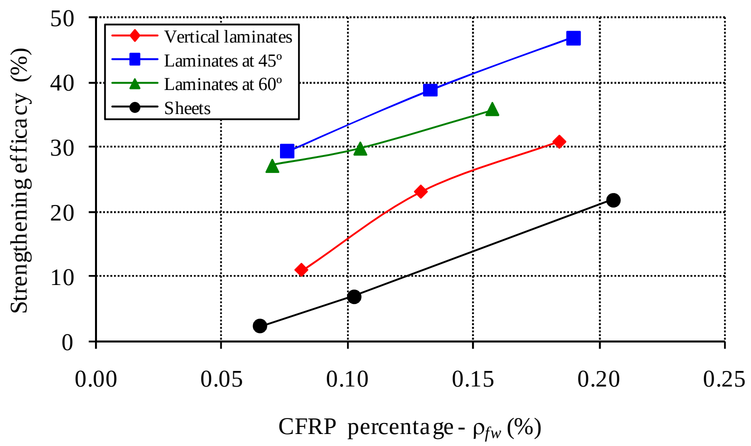

Figure 6: Strengthening efficacy ($\Delta F_{max}/F_{max}^{2S-R}$) *vs* CFRP percentage ($\rho_{fw}$)

2.4.4 Strains in the CFRP and steel stirrups

Figure 7 represents the relationship between ε_{CFRP}^{max} and ρ_{fw} (thick line) and between $(\varepsilon_{CFRP}^{max})_{med}$ and ρ_{fw} (dashed line), where ε_{CFRP}^{max} is the maximum strain recorded up to the maximum load of the beams, amongst the strain values registered in the strain gauges installed in the monitored laminates and strips (see Figures 2 and 3), and $(\varepsilon_{CFRP}^{max})_{med}$ is the average strain of the maximum strain values registered in the monitored CFRP (two per beam). It can be verified that ε_{CFRP}^{max} in the laminates ranged from 5.6‰ in the 2S-4LV beam and 10.8‰ in the 2S-4LI45. In terms of $(\varepsilon_{CFRP}^{max})_{med}$, the variation was between 5.5‰ in the 2S-4LV and 10.3‰ in the 2S-4LI45. Apart the beams with vertical laminates, both ε_{CFRP}^{max} and $(\varepsilon_{CFRP}^{max})_{med}$ decreased with the increase of ρ_{fw}. This can be justified by the crack pattern and failure modes occurred. In fact, with the increase of ρ_{fw} the crack pattern was more diffuse and the concrete cover that includes the laminates had a tendency to separate from the concrete core of the beams, resulting more uniform strain distributions along the CFRP elements, but the probability of occurring high gradients of strains, typical of beams with low ρ_{fw}, is reduced. Figure 7 shows that the maximum values for the ε_{CFRP}^{max} and $(\varepsilon_{CFRP}^{max})_{med}$ were recorded in the NSM beams, while the minimum values were registered in the EBR beams. The abnormal low values for the beams with the minimum ρ_{fw} of vertical laminates are justified by the failure mode occurred. In fact, in the 2S-4LV beam the bond length of the laminates crossed by the shear failure crack was too reduced (see Figure 5). In the case of the 2S-7LV beam (intermediate ρ_{fw}) the laminate that offered the highest contribution for the shear resistance was not monitored (see Figures 2 and 5).

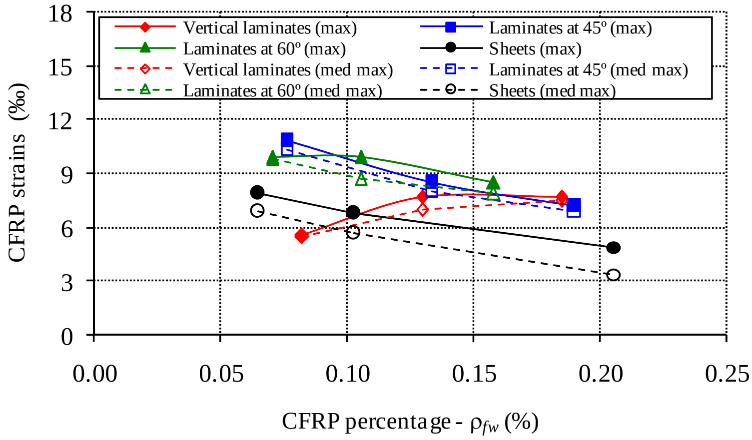

Figure 7: CFRP strains *vs* CFRP percentage (ρ_{fw})

3 CONCLUSIONS

In the present paper the effectiveness of the EBR and NSM techniques for the shear strengthening of T cross section RC beams was compared. For this purpose an experimental program was carried out. The effectiveness of the techniques was appraised from the contribution provided by the distinct CFRP shear strengthening arrangements in terms of load carrying capacity, stiffness of the response of the beams after the formation of the shear failure crack in the reference beam, maximum strains measured in the CFRP and failure modes. In the case of NSM beams, the influence of the percentage and inclination of the laminates was evaluated.

From the obtained results it can be concluded that NSM technique is much more efficient that EBR, since it provides a larger increase in terms of maximum load, load carrying capacity after shear crack formation and maximum strains in the CFRP materials. Moreover, NSM is simpler and faster to apply than EBR. However, it seems that a limit exists for the spacing between laminates since for the maximum percentage of laminates a failure mode consisting on the detachment of the concrete cover of the beams lateral faces occurred, leading to a lost of effectiveness of the technique. In terms of the NSM beams, the most effective inclination of laminates was 45º, independent of the percentage of laminates. Laminates at 60º were more effective than vertical laminates. For the range of CFRP percentage values (ρ_{fw}) considered in this work, a trend of linear increasing of the shear strengthening efficacy ($\Delta F_{max}/F_{max}^{2S-R}$) with the increase of ρ_{fw} was verified. The highest percentage of CFRP was designed to provide a maximum load similar to that of the 7S-R beam, with a reinforcing system composed of seven steel stirrups. Although the beams with the highest percentage of NSM laminates had an average value of the maximum load (P_{max}) equal a 0.9P_{max} of the 7S-R beam, the NSM CFRP laminates shear strengthened beams presented higher stiffness, mainly after shear crack initiation, which did not occur in EBR beam with the highest percentage of CFRP.

ACKNOWLEDGMENTS

The authors wish to acknowledge the support provided by the "Empreiteiros Casais", Degussa, S&P® and Secil (Unibetão, Braga). The study reported in this paper forms a part of the research program "SmartReinforcement - Carbon fibre laminates for the strengthening and monitoring of reinforced concrete structures" supported by ADI-IDEIA, Project nº 13-05-04-FDR-00031.

REFERENCES

[1] De Lorenzis, L. and Nanni, A., "Shear Strengthening of Reinforced Concrete Beams with Near-Surface Mounted Fiber-Reinforced Polymer Rods", *ACI Structural Journal*, Vol. 98, Nº. 1, pp. 60-68 (2001).

[2] Carolin, A., "Carbon fibre reinforced polymers for strengthening of structural elements", PhD thesis, Lulea University of Technology (2003).

[3] Nanni, A., Di Ludovico, M. and Parretti, R., "Shear strengthening of a PC bridge girder with NSM CFRP rectangular bars", *Advances in Structural Engineering*, Vol. 7, Nº. 4, pp. 97-109 (2004).

[4] Barros, J.A.O., Dias, S.J.E. and Lima, J.L.T., "Efficacy of CFRP-based techniques for the flexural and shear strengthening of concrete beams", *Journal Cement and Concrete Composites*, 29(3), 203-217 (2007).

[5] Barros, J.A.O. and Dias, S.J.E., "Near surface mounted CFRP laminates for shear strengthening of concrete beams", *Journal Cement and Concrete Composites*, Vol. 28, N. 3, pp. 276-292 (2006).

[6] Dias, S.J.E. and Barros, J.A.O., "NSM CFRP Laminates for the Shear Strengthening of T Section RC Beams", 2nd International fib Congress, Naples, Italy, Paper ID 10-58 in CD (2006).

[7] De Lorenzis, L. and Rizzo, A., "Behaviour and capacity of RC beams strengthened in shear with NSM FRP reinforcement", 2nd International fib Congress, Naples, Italy, Paper ID 10-9 in CD (2006).

[8] Dias, S.J.E., Bianco, V., Barros, J.A.O. and Monti, G., "Low strength T-cross section RC beams shear-strengthened by NSM technique", Materiali ed Approcci Innovativi per il Progetto in Zona Sismica e la Mitigazione della Vulnerabilità delle Strutture Università degli Studi di Salerno - Consorzio ReLUIS, paper 007 (2007).

[9] ACI Committee 440, "Guide for the design and construction of externally bonded FRP systems for strengthening concrete structures", American Concrete Institute, 118 pp. (2002).

[10] Sena-Cruz, J.M. and Barros, J.A.O., "Bond between near-surface mounted CFRP laminate strips and concrete in structural strengthening", *Journal of Composites for Construction*, 8(6), p. 519-527 (2004).

[11] EN 206-1, "Concrete - Part 1: Specification, performance, production and conformity." European standard, CEN, 69 pp. (2000).

[12] EN 10002-1, *Metallic materials - Tensile testing. Part 1: Method of test (at ambient temperature)*, European Standard, CEN, Brussels, Belgium, 35 pp. (1990).

[13] ISO 527-5, *Plastics - Determination of tensile properties - Part 5: Test conditions for unidirectional fibre-reinforced plastic composites*, International Organization for Standardization (ISO), Geneva, Switzerland, 9 pp. (1997).

[14] Barros, J.A.O. and Ferreira, D.R.S.M., "Assessing the efficiency of CFRP discrete confinement systems for concrete column elements", *Journal of Composites for Construction*, 12(2), March/April (2008).

[15] Bianco, V., Barros, J.A.O. and Monti, G., "Influence of the Concrete Mechanical Properties on the Efficacy of the Shear Strengthening Intervention on RC Beams by NSM Technique", Asia-Pacific Conference on FRP in Structures (APFIS 2007), Hong Kong, China (2007).